Developmental Biology
Neuroscience

Embryonic origins of forebrain oligodendrocytes revisited by combinatorial genetic fate mapping

Reviewed Preprint
v2 • July 2, 2024
Revised by authors

Reviewed Preprint
v1 • April 10, 2024

Yuqi Cai, Zhirong Zhao, Mingyue Shi, Mingfang Zheng, Ling Gong, Miao He

Institutes of Brain Science, State Key Laboratory of Medical Neurobiology and MOE Frontiers Center for Brain Science, Department of Neurobiology, Zhongshan Hospital, Fudan University, Shanghai 200032, China

Abstract

Multiple embryonic origins give rise to forebrain oligodendrocytes (OLs), yet controversies and uncertainty exist regarding their differential contributions. We established intersectional and subtractional strategies to genetically fate map OLs produced by medial ganglionic eminence/preoptic area (MGE/POA), lateral/caudal ganglionic eminences (LGE/CGE) and dorsal pallium. We found that, contrary to the canonical view, LGE/CGE-derived OLs make minimum contributions to the neocortex and corpus callosum, but dominate piriform cortex and anterior commissure. Additionally, MGE/POA-derived OLs, instead of being entirely eliminated, make small but sustained contribution to cortex with a distribution pattern distinctive from those derived from the dorsal origin. Our study provides a revised and more comprehensive view of cortical and white matter OL origins, and established valuable new tools and strategies for future OL studies.

eLife assessment

In this study the authors revisited the question of the embryonic origin of telencephalic oligodendrocytes using some new and powerful genetic tools. There is **convincing** evidence to support previous suggestions of a predominantly cortical origin of oligodendrocytes in the cerebral cortex. The findings are **valuable** and should be of interest to developmental and myelin biologists.

https://doi.org/10.7554/eLife.95406.2.sa3

Introduction

Oligodendrocytes (OLs) are an important class of macroglia responsible for producing the myelin sheaths that insulate and protect neuronal axons. Forebrain OLs arise from multiple embryonic origins. Previous fate mapping study using *Nkx2.1*^{Cre}[1], *Gsh2*^{Cre}[2] and *Emx1*^{Cre}[3] reported consecutive and competing waves of OLs derived from medial ganglionic eminence/preoptic area (MGE/POA), lateral/caudal ganglionic eminences (LGE/CGE) and dorsal pallium[2]. The first-wave of OLs generated by MGE/POA ($_{MP}$OLs) were believed to be

eliminated postnatally, while those from the second and third waves ($_{LC}$OLs and dOLs) survive and populate the cortex and corpus callosum at comparable proportions. Several other studies provided both supporting and contradicting evidence to this model[4–11]. Moreover, *Gsh2* was recently found to be expressed in dorsal progenitors[12], casting doubt on the interpretation of lineage tracing data from $Gsh2^{Cre}$.

In this study, we generated new genetic tools and combinatorial fate mapping strategies which allow direct visualization and comparison among OLs derived from different origins. We found that neocortical OLs are primarily composed of dOLs, rather than similar proportions of $_{LC}$OLs and dOLs. In contrast, $_{LC}$OLs and dOLs made comparable contributions to piriform cortex. We also found that although $_{MP}$OLs only make a small contribution, they do persist in the cortex beyond adulthood with a unique spatial pattern distinct from that of the dOLs. In the two major white matter commissure tracts, dOLs are the vast majority in corpus callosum but make little contribution to anterior commissure, while $_{LC}$OLs behaved the opposite. These findings significantly revised the classical view and provided a new and more comprehensive picture of cortical and white matter OL origins.

Results and Discussion

To unambiguously track OLs from different embryonic origins, we first generated a knock-in driver, $Opalin^{P2A\text{-}Flpo\text{-}T2A\text{-}tTA2}$ (**Figure 1**), orthogonal to Cre drivers that label dorsal or ventral progenitors ($Progenitor^{Cre}$). *Opalin* (also known as *Tmem10*) encodes oligodendrocytic myelin paranodal and inner loop protein that are specifically expressed in differentiated oligodendrocytes[13–16]. In $Opalin^{P2A\text{-}Flpo\text{-}T2A\text{-}tTA2}$, *Flpo* and *tTA2* were inserted before the STOP codon and linked by self-cleavage peptide P2A and T2A (**Figure 1A-C**), allowing co-transcription and translation with *Opalin*. Flp-mediated recombination by this driver (hereinafter referred to as $Opalin^{Flp}$for simplicity) enables highly specific, efficient and irreversible OL labeling, while the tTA2 component offers the flexibility for OL-specific labeling in tunable densities (**Figure 1D-F**).

Next, we established two types of genetic combinatorial fate mapping strategies to directly visualize OLs from different embryonic origins (**Figure 2**): (1) combining $Opalin^{Flp}$ and $Progenitor^{Cre}$ with intersectional reporters *Ai65* to label OLs derived from Cre+ progenitor domain by RFP (**Figure 2A**); (2) combining $Opalin^{Flp}$ and $Progenitor^{Cre}$ with *RC::FLTG*[17] to simultaneously label OLs derived from Cre+ progenitors by GFP and OLs derived from the complementing Cre-progenitors by RFP (**Figure 2B**, Supplementary Figure 1A). The first approach allowed us to track dOLs and $_{MP}$OLs (**Figure 2C**, E). The second approach empowered us to observe and compare OLs generated from dorsal and ventral origins (Supplementary Figure 1B), or those from Gsh2+ and Gsh2-progenitors, in the same brain (Supplementary Figure 1C). Importantly, the subtraction power enabled us to target OLs derived from LGE/CGE progenitors that express neither *Emx1* nor *Nkx2.1* (**Figure 2D** and Supplementary Figure 1D). In addition, these strategies greatly facilitated the identification of OLs derived from specific origin which exist at relatively low density in certain regions.

Deploying these strategies, we assessed the differential contributions of dOLs, $_{LC}$OLs and $_{MP}$OLs by analyzing RFP+ cells in the following mice: $Opalin^{Flp}$::$Emx1^{Cre}$::*Ai65* (**Figure 2C**), $Opalin^{Flp}$::$Emx1^{Cre}$::$Nkx2.1^{Cre}$::*RC::FLTG* (**Figure 2D**) and $Opalin^{Flp}$::$Nkx2.1^{Cre}$::*Ai65* (**Figure 2E**). To better assess their contributions to the total OL population (**Figure 2F**), we co-stained RFP with the mature OL marker aspartoacylase (ASPA)[18] (**Figure 2G-I**) and quantified the ratio of colocalization (**Figure 2J**). Notably, all RFP+ cells are ASPA+, reassured the specificity of our label strategies. We observed two significant differences from the traditional model in the neocortex. The first major deviation is that, instead of comparable contributions by dOLs and $_{LC}$OLs, the vast majority of neocortical OLs were dOLs but not $_{LC}$OLs. The densities (**Figure 2G-I**

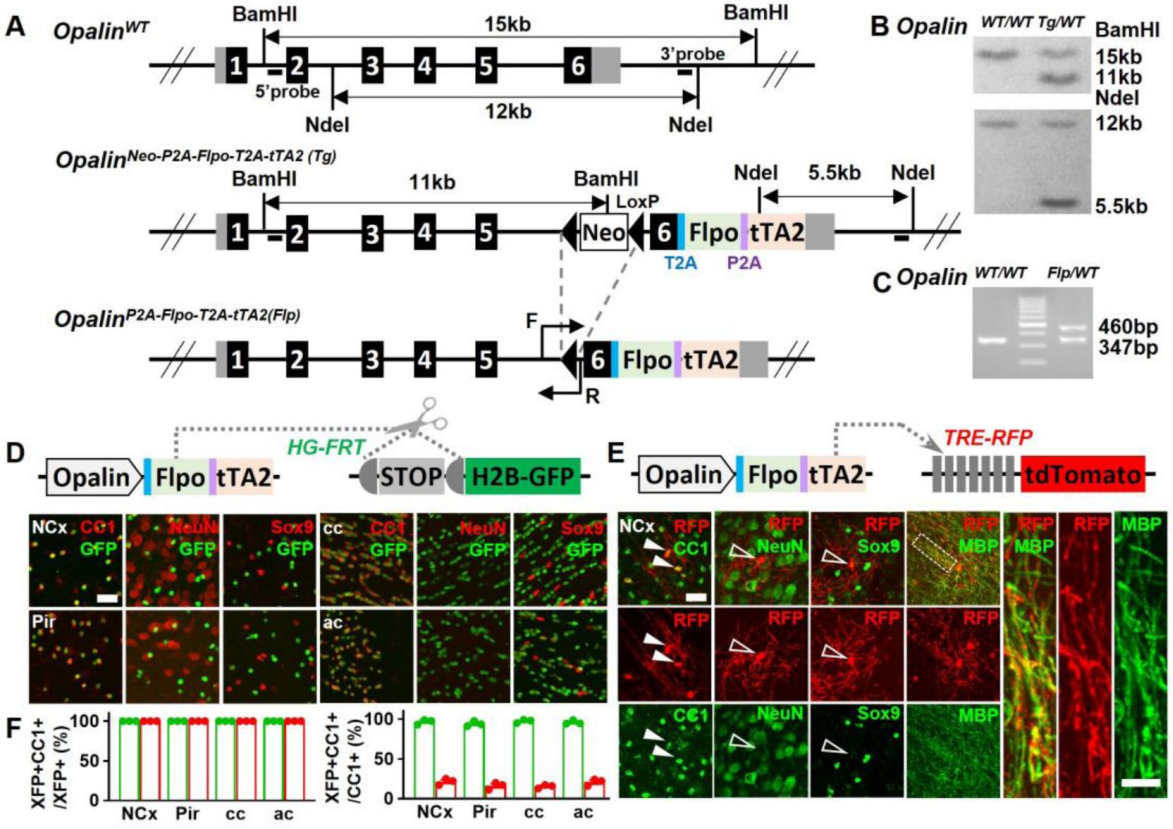

Figure 1.

A new driver mouse for efficient and specific OL labeling

(**A**) Scheme for generating the *Opalin*$^{P2A\text{-}Flpo\text{-}T2A\text{-}tTA2}$allele. **(B)** Southern blot confirmation of correctly targeted ES clone. **(C)** Genomic PCR to genotype F1 offspring. **(D)** OL labeling by Flp. **(E)** OL labeling by tTA2. High magnification images of the boxed region showing co-localization of RFP with MBP staining, which further demonstrated the myelination ability of labeled OLs. **(F)** Quantification of labeling specificity (left panel) and efficiency (right panel) by colacalization with OL marker CC1. Both reporting systems are highly specific, as shown by the complete co-localization of fluorescent protein (XFP) with OL marker (CC1) and lack of co-staining with neuronal marker (NeuN) or astrocyte marker (Sox9). Quantification bar-graph was not presented for NeuN and Sox9 as zero co-localizations were observed in all analyzed regions. Close to complete OL labeling was achieved by Flp-dependent H2B-GFP reporter in all analyzed regions (green dots), while sparser labeling with variable regional density was achieved by tTA2-dependent tdTomato reporter driven by TRE promoter (red dots). NCx: neocortex. Pir: piriform cortex. cc: corpus callosum. ac: anterior commissure. Scale bar: 50 μm in low magnification images, 5μm in high magnification images. Quantification: n=3. Dots represent data from individual mice.

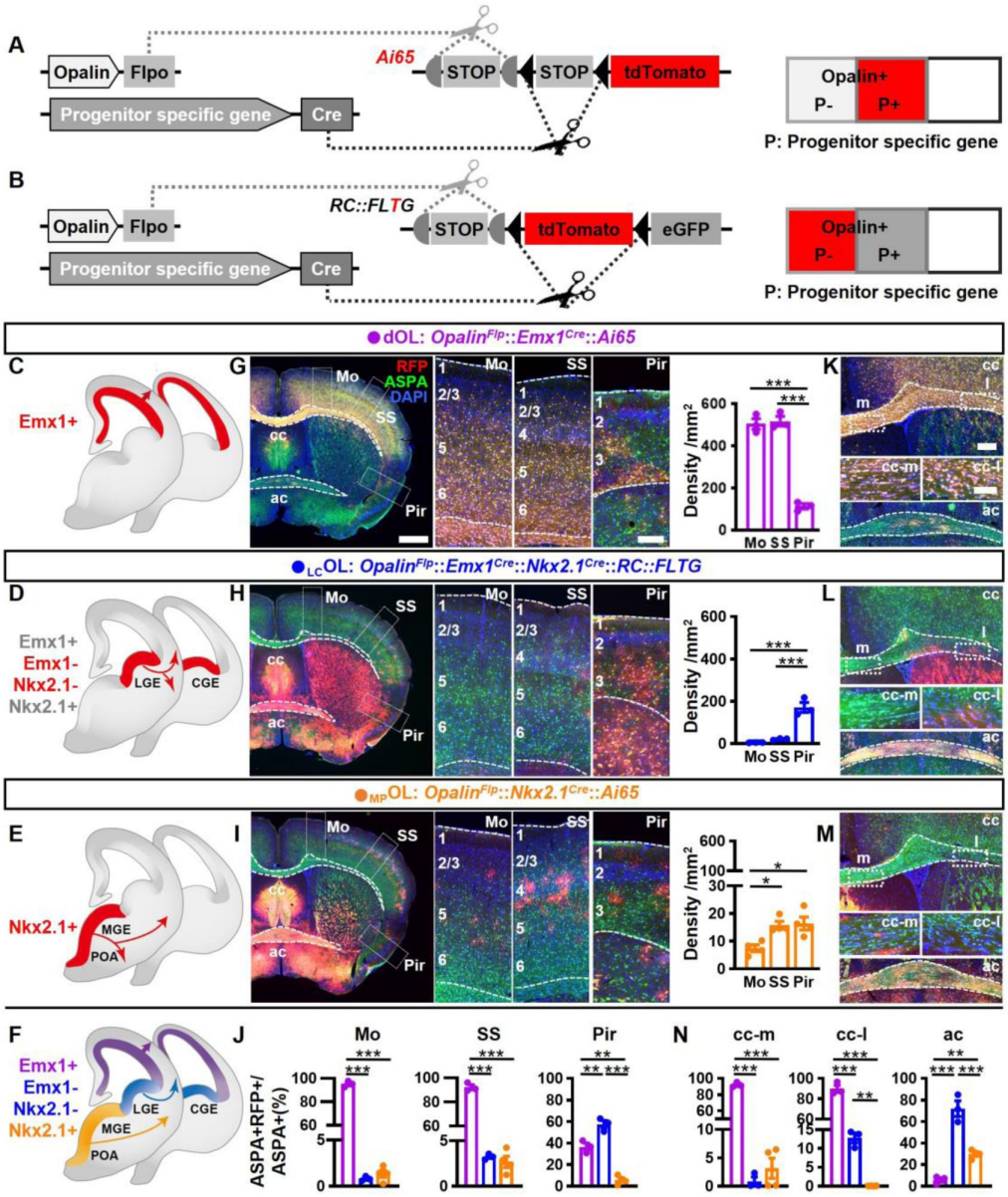

Figure 2.

Combinatorial fate mapping of dOLs, $_{MP}$OLs and $_{LC}$Ols

(**A**) Strategy for intersectional labeling. Flp-AND-Cre labels OLs from Cre-expressing progenitors with RFP. **(B)** Strategy for subtractional labeling of OLs derived from non-Cre-expressing progenitors with RFP. The eGFP expressing OLs derived from Cre expressing progenitors were not used for analysis in this scenario and thereby were not highlighted by color. **(C-F)** Schematics showing intersectional labeling of dOLs in *Opalin^{Flp}::Emx1^{Cre}::Ai65* (C), subtractional labeling of $_{LC}$OLs in *Opalin^{Flp}::Emx1^{Cre}::Nkx2.1^{Cre}::RC::FLTG* (D), intersectional labeling of $_{MP}$OLs in *Opalin^{Flp}::Nkx2.1^{Cre}::Ai65* (E) and cortical OLs derived from all three origins (F). **(G-I)** Representative images (left panels) and quantifications (right panels) of RFP+ cell density in motor cortex (Mo), somatosensory cortex (SS) and piriform cortex (Pir). **(J)** Quantification of differential contribution to ASPA+ OLs by three embryonic origins to Mo, SS and Pir. **(K-N)** Representative images (K-M) and quantifications (N) of differential contribution to ASPA+ OLs by three embryonic origins in the two major commissure white matter tracts: corpus callosum(cc) and anterior commissure (ac). $_{MP}$OLs and $_{LC}$OLs preferentially reside in the medial and lateral cc (cc-m and cc-l), respectively. Scale bar: 1mm in low magnification images in (G-I), 250 μm in high magnification images of the boxed area in (G-I) and low magnification images in (K-M), 100 μm in high magnification images of the boxed area (cc-m and cc-l) in (K-M). n=3 for dOLs and $_{LC}$OLs; n=4 for $_{MP}$OLs. Dots represent data from individual mice. Error bar: S.E.M. *P < 0.05, **P < 0.01, ***P < 0.001.

and Supplementary Figure 2A-F) and ASPA ratios (**Figure 2J**) of dOLs are much higher than those of $_{LC}$OLs. Considering the possibility of incomplete recombination in combinatorial reporters, and the relatively low Cre activity in the dorsal MGE of *Nkx2.1*^{Cre}[1], the genuine contribution of $_{LC}$OLs to the neocortex could be even lesser than our current observation. Therefore, the large quantity of neocortical OLs labeled by *Gsh2*^{Cre}in previous study[2] or by GFP in *Opalin*^{Flp}::*Gsh2*^{Cre}::*RC::FLTG* (Supplementary Figure 1C) most likely were predominantly dOLs generated by Gsh2+ dorsal progenitors[12], rather than bona fide $_{LC}$OLs.

The second major deviation is that cortical $_{MP}$OLs are not completely depleted postnatally. Instead, they make a small but continued contribution with a unique spatial distribution pattern (**Figure 2I-J** and Supplementary Figure 2D-G). $_{MP}$OLs display a clear rostrocaudal density decline (Supplementary Figure 2E-F), a higher density in somatosensory cortex (SS) than motor cortex (Mo) (**Figure 2I**), and a laminar preference towards layer 4 (L4) in SS (Supplementary Figure 2G). In contrast, the distribution of dOLs and $_{LC}$OLs do not vary significantly across the rostrocaudal axis (Supplementary Figure 2E-F) or between Mo and SS (**Figure 2G-H**), but exhibits increased density towards deeper layers (Supplementary Figure 2G). Importantly, we have observed cortical $_{MP}$OLs in mice as old as one year (Supplementary Figure 2H), well beyond the age analyzed in previous reports[2, 7, 8], suggesting a persisted contribution.

We then turned our attention to the lateral three-layer archicortex, piriform cortex (Pir). Different from the neocortex, Pir contains higher proportions (**Figure 2J**) of $_{LC}$OLs than dOLs. $_{MP}$OLs make the lowest contribution (**Figure 2J**) at a density similar to SS and higher than Mo (**Figure 2I**).

These combinatorial models also grant us the opportunity to revisit the differential contributions of dOLs, $_{LC}$OLs and $_{MP}$OLs to the two commissural white matter tracts, corpus callosum (cc) and anterior commissure (ac), which contain high density of OLs (**Figure 2K-M**). We found that, similar to the neocortex, cc is mainly populated by dOLs and supplemented by very low proportions of $_{LC}$OLs and $_{MP}$OLs (**Figure 2K-N**). Interestingly, $_{LC}$OLs and $_{MP}$OLs seem to show preferential distribution in the lateral and medial regions of cc (cc-l and cc-m), respectively (**Figure 2L-N**). Different from cc, ac is mainly populated by $_{LC}$OLs and $_{MP}$OLs and supplemented by very low proportion of dOLs (**Figure 2K-N**).

To substantiate the above results, we further breed *Opalin*^{Flp}::*Emx1*^{Cre}::*Nkx2.1*^{Cre}::*Ai65* to label dOLs together with $_{MP}$OLs by RFP and co-stained them with ASPA (Supplementary Figure 3). RFP-ASPA+ cells were difficult to find in Mo, SS and cc, but were more easily observed in Pir and ac, consistent with the respective low and high $_{LC}$OL contributions in these regions.

In summary, our findings significantly revised the canonical model of forebrain OL origins (**Figure 3A**), and provided a new and more comprehensive view (**Figure 3B**). We demonstrated that neocortical OLs are mainly derived from dorsal origin with small but lasting contribution from the ventral origin (**Figure 2**, Supplementary Figure 1B and 2). Our data showed that LGE/CGE makes little contribution to neocortex and cc, but makes major contribution to piriform cortex and ac (**Figure 2** and Supplementary Figure 3). This finding is supported by another report in which in utero electroporation failed to label LGE-derived cortical OLs in both embryonic and early postnatal brains, and an exclusion strategy revealed very low percentage of LGE/CGE-derived cortical OLs in neonatal brains[19]. The lack of adult labeling in our study together with the lack of developmental labeling in the other study suggest that the lack of $_{LC}$OL in neocortex is less likely caused by competitive postnatal elimination, but more likely due to limited production and/or allocation. We further discovered that MGE/POA makes a small but persistent contribution to the neocortex with a distinct distribution pattern featured by a rostral-high to caudal-low gradient and a preference towards L4 in SS (Supplementary Figure 2). Whether their enduring existence and highly biased localization has functional implications awaits future exploration. In addition, we found that the cc showed a similar OL composition as the neocortex, but the Pir and the ac each

exhibited distinct OL compositions in term of their embryonic origins. $_{LC}$OLs are the major contributor to both regions, while dOLs and $_{MP}$OLs mainly contribute to Pir and ac, respectively (**Figure 2**).

In addition to the new framework of forebrain OL origins (**Figure 3**), we also generated a new driver (**Figure 1**) and established multiple combinatorial genetic models (**Figure 2**) for efficient tracking and direct visualization of OLs from different embryonic origins without interference from other cells types sharing the same progenitor domains such as oligodendrocyte precursors, astrocytes, and neurons (**Figure 1**-**2**). These tools set up a firm foundation and will provide reliable experimental access for future inquiries on the development and function of diverse OLs in healthy and disease brains[20], especially to uncover the relationship between their developmental origins and the functional and molecular heterogeneity.

Material and Methods

Mice

All mouse studies were carried out in strict accordance with the guidelines of the Institutional Animal Care and Use Committee of Fudan University. All husbandry and experimental procedures were reviewed and approved by the same committee. All applicable institutional and/or national guidelines for the care and use of animals were followed. The following transgenic mouse lines were used in this study: *Nkx2.1^{Cre}* (Jax 008661)[1],*Gsh2^{Cre}*(Jax 025806)[2], *Emx1^{Cre}* (Jax 005628)[3], *Ai65* (Jax 021875)[21], *RC::FLTG* (Jax 026932)[17]. The tTA2-dependent tdTomato reporter (*TRE-RFP*) was derived from *Ai62* (Jax 022731) [21], by removing LoxP-STOP-LoxP with *E2a-Cre* (Jax 003724). The Flp dependent H2B-GFP reporter (*HG-FRT*) was derived from *HG-dual* (Jax 028581) via removal of loxP flanking STOP cassette by *CMV-Cre*[22]. The *Opalin$^{P2A\text{-}Flpo\text{-}T2A\text{-}tTA2}$* allele was generated by targeted insertion of the T2A-Flpo-P2A-tTA2 sequence immediately before the STOP codon of the endogenous *Opalin* gene using homologous recombination. Gene targeting vector was generated using PCR-based cloning approach as described before[22]. More specifically, a 4.7 kb 5' homology arm, a loxP flanking Neo positive selection cassette, a T2A-Flpo-P2A-tTA2 cassette and a 2.7 kb 3' homology arm were cloned into a building vector containing the DTA negative selection cassette to generate the targeting vector. Targeting vector was linearized and transfected into a C57/black6 ES cell line. ES clones that survived through negative and positive selections were first screened by genomic PCR, then confirmed by Southern blotting using appropriate DIG-dUTP labelled probes. One positive ES cell clone was used for blastocyst injection to obtain male chimera mice carrying the modified allele following standard procedures. Chimera males were bred with C57BL/6J females to confirm germline transmission by genomic PCR. The Neo selection cassette was self-excised during spermatogenesis of F0 chimeras. Heterozygous F1 siblings were bred with one another to establish the colony. Targeting vector construction, ES cell transfections and screening, blastocyst injections and chimera breeding were performed by Cyagen.

Genomic PCR

Genomic DNA was prepared from mouse tails. Tissue was lysed by incubation in tail lysis buffer (Viagen, 102-T) with 0.1 mg/ml proteinase K (Diamond, A100706) overnight at 55°C followed by 45 min at 90°C in an air bath to inactivate proteinase K. The lysate was cleared by centrifugation at maximum speed (21,130 G) for 15 min in a table-top centrifuge. Supernatant containing genomic DNA was used as the PCR template for amplifying DNA products. The following primers were used:

Opalin-F: 5'-GGCCTATGTTTGATTTCCAGCACTG –3'

Opalin-R: 5'-AGCACTTATGACTGCTGAGCCGTTC –3'

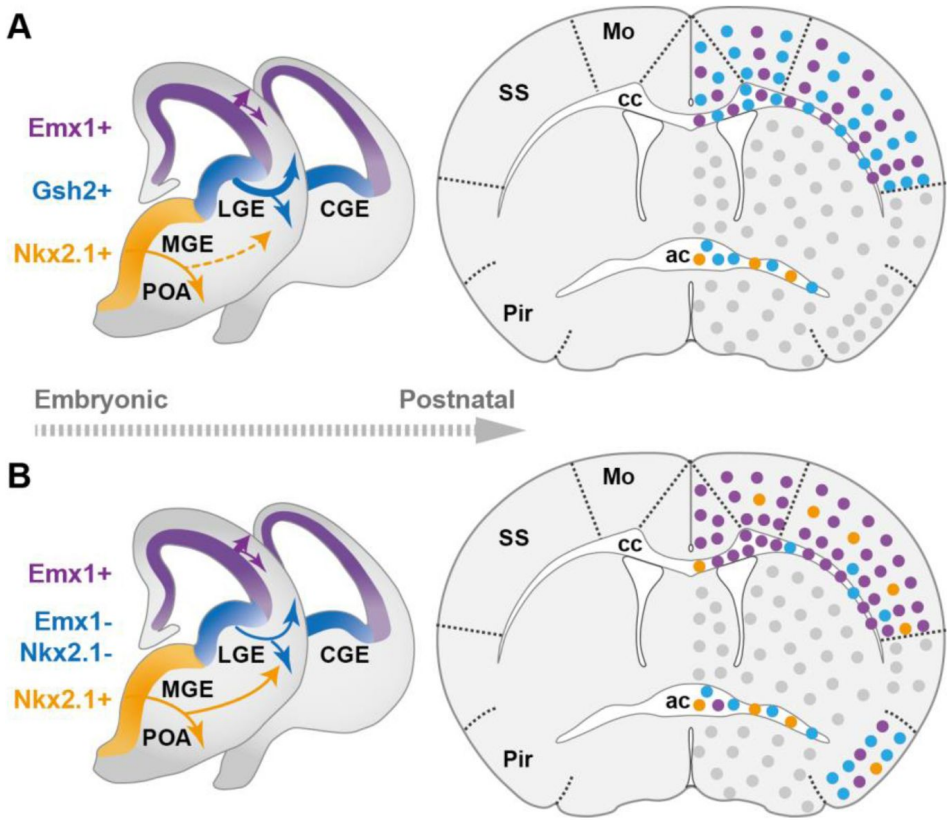

Figure 3.

The classical and revised model of forebrain OL origins

(**A**) In the classical model[2], OLs derived from MGE/POA (orange) were largely eliminated postnatally (thin dashed line), while those from LGE/CGE (blue) and dorsal origin (purple) survive at similar proportions (thick solid line). Therefore, neocortex (NCx) and corpus callosum (cc) contain comparable density of $_{LC}$OLs (blue dots) and dOLs (purple dots) and are devoid of $_{MP}$OLs (orange dots). **(B)** In the new model, NCx and cc mainly contains dOLs with very low contribution from the ventral origins. $_{LC}$OLs mainly contribute to piriform cortex (Pir) and anterior commissure (ac). $_{MP}$OLs makes a small but sustained contribution to NCx, with a strong laminar preference towards layer 4 in somatosensory cortex (SS). In addition, dOLs and $_{MP}$OLs also make substantial contributions to Pir and ac, respectively. Grey dots indicate OLs in unanalyzed regions.

Immunohistochemistry and microscopy

Mice were anaesthetized by intraperitoneal injection of 1.5% sodium pentobarbital (0.09 mg/g body weight) and then intracardially perfused with saline followed by 4% paraformaldehyde in 0.1 M PB. Following post fixation at 4°C for 24 hours, brain samples were sectioned at 30 μm using a vibratome (Leica VT1000S), or transferred into 30% sucrose in 0.1M PB for cryoprotection, OCT embedded, and sectioned using a cryostat (Leica CM1950). For CC1 immunostaining, antigen retrieval was performed prior to blocking by boiling for 3 min in 10 mM citrate buffer (pH6.0). Sections were blocked in PBS containing 0.05% Triton and 5% normal donkey serum and then incubated with the following primary antibodies in the blocking solution at 4 ℃ overnight: RFP (goat polyclonal antibody, 1:2000, SICGEN AB0081-200; rabbit polyclonal antibody, 1:2000, Rockland 600-401-379), GFP (chicken polyclonal antibody, 1:1000, Aves Labs, GFP-1020), MBP (rat polyclonal antibody, 1:500, AbD Serotec, MCA409S), CC1 (rabbit polyclonal antibody, 1:500, Oasis Biofarm, OB-PRB070, mouse polyclonal antibody, 1:300, Millipore, OP80), ASPA (rat polyclonal antibody, 1:200, Oasis Biofarm, OB-PRT005), Sox9(rabbit polyclonal antibody, 1:2000, Chemicon, AB5535), NeuN (mouse monoclonal antibody, 1:500, Millipore, MAB377). Sections were then incubated with appropriate Alexa fluor dye-conjugated IgG secondary antibodies (1:500, Thermofisher Scientific) or CF dye-conjugated IgG secondary antibodies (1:250, Sigma) in blocking solution and mounted in Aqua-mount (Southern Biotech, 0100-01). Sections were counterstained with DAPI. Sections were imaged with confocal microscopy (Olympus FV3000), fluorescence microscopy (Nikon Eclipse Ni; Olympus VS120; Olympus VS200) and fluorescent stereoscope (Nikon SMZ25). All quantifications were performed in 2-month-old adult mice from coronal sections between Bregma +1.94 and –2.80 mm. Anatomical regions were identified according to the *Paxinos "The Mouse Brain" Atlas* and the *Allen Reference Atlas*, and their areas were measured in ImageJ for density calculations, whenever applicable. For cortical regions, every fourth section within the range of selection was analyzed. For whiter matter tracts, three consecutive sections at Bregma 0.14 were analyzed. At least three brains were analyzed for each genotype. To quantify density and co-localization, cells were identified and counted in Adobe Photoshop or Image J in conjugation with QuPath.

Statistical analysis

GraphPad Prism version 8.0.1 was used for statistical calculations. No statistical methods were used to predetermine sample sizes, but our sample sizes are similar to those reported in previous publications. Data collection and analysis were performed blind to the conditions of the experiments whenever possible. No animals or data points were excluded from the analysis. Normalcy was assessed using Shapiro-Wilk test. Equal variances were assessed using F test or Bartlett's test. Statistical significance was tested using two-tailed unpaired t-test, Welch's t-test, one-way ANOVA and two-way ANOVA followed by Tukey's or Bonferroni post hoc test, wherever appropriate. Data are presented as mean ± standard error of the mean (S.E.M.). $P < 0.05$ was considered significant. Significance is marked as *$P < 0.05$; **$P < 0.01$ and ***$P < 0.001$.

Acknowledgements

We thank Dr. Yilin Tai for helpful discussion and Dr. Min Jiang from core facility of IOBS, Fudan University, for technical support on imaging experiments. This study was supported by funds from the National Science and Technology Innovation 2030 Major Projects of China (STI2030-Major Projects-2022ZD0206500), National Natural Science Foundation of China (32171087, 32200918, 32371145).

Author contributions

Conceptualization: MH

Methodology: YC, MH

Investigation: YC, ZZ, MS

Visualization: YC, MH, LG

Supervision: MH, LG

Writing—original draft: MH, YC, LG

Writing—Review and editing: MH, YC, ZZ, MZ

Declaration of interests

The authors declare no competing interests.

Supplementary information

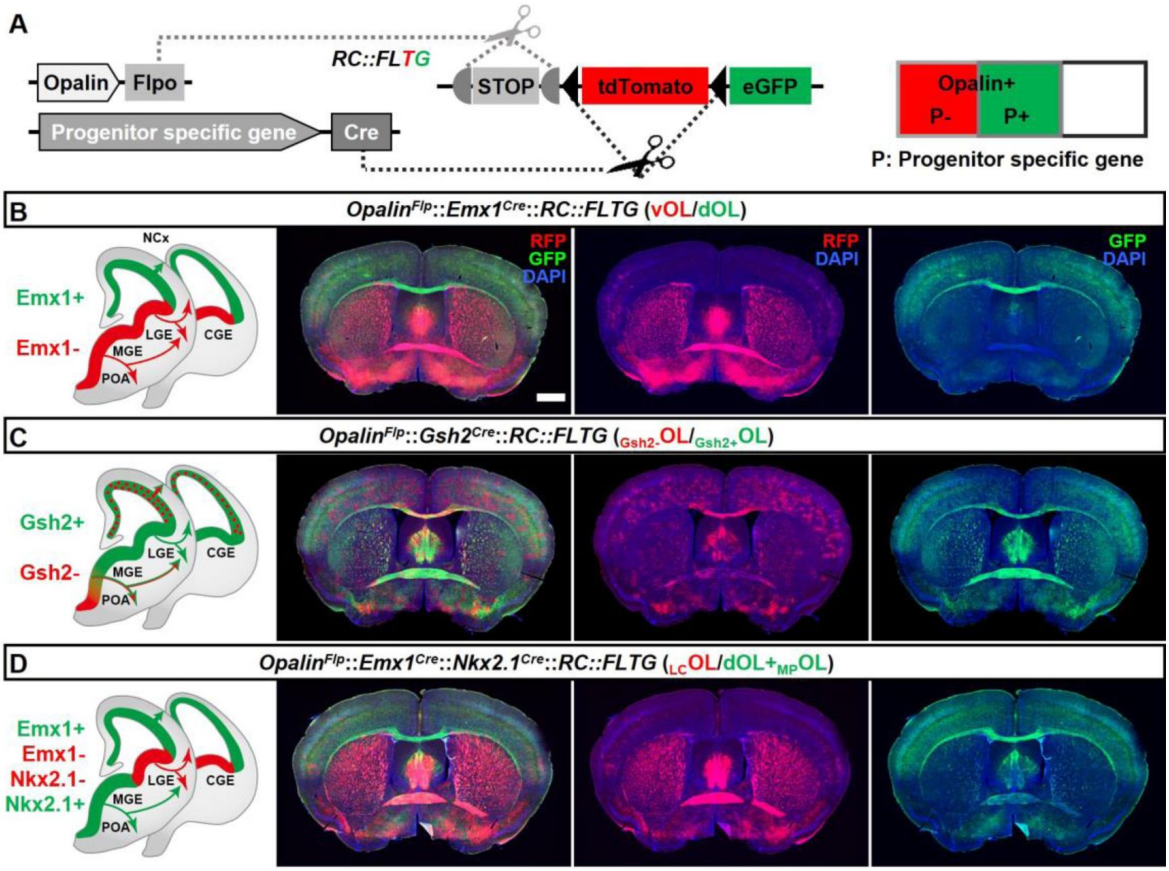

Supplementary Figure 1.

Simultaneous differential labeling of OLs derived from complementary embryonic origins

(**A**) Strategy for simultaneous labeling of OLs derived from complementary origins. Flp-NOT-Cre labels OLs from non-Cre-expressing progenitors with RFP, while Flp-AND-Cre labels OLs from Cre-expressing progenitors with eGFP. **(B)** Coronal sections showing GFP+ OLs from dorsal origin (dOLs) and RFP+ OLs from ventral origin (vOLs) in *Opalin^{Flp}::Emx1^{Cre}::RC::FLTG.* **(C)** Coronal sections showing GFP+ OLs derived from Gsh2+ progenitors ($_{Gsh2+}$OL) and RFP+ OLs derived from Gsh2- progenitors ($_{Gsh2-}$OL) in *Opalin^{Flp}::Gsh2^{Cre}::RC::FLTG.* **(D)** Coronal sections showing GFP+ OLs from dorsal and MGE/POA origin (dOLs+$_{MP}$OLs) and RFP+ OLs from LGE/CGE origin ($_{LC}$OLs) in *Opalin^{Flp}:: Emx1^{Cre}:: Nkx2.1^{Cre}::RC::FLTG.* Scale bar: 1mm.

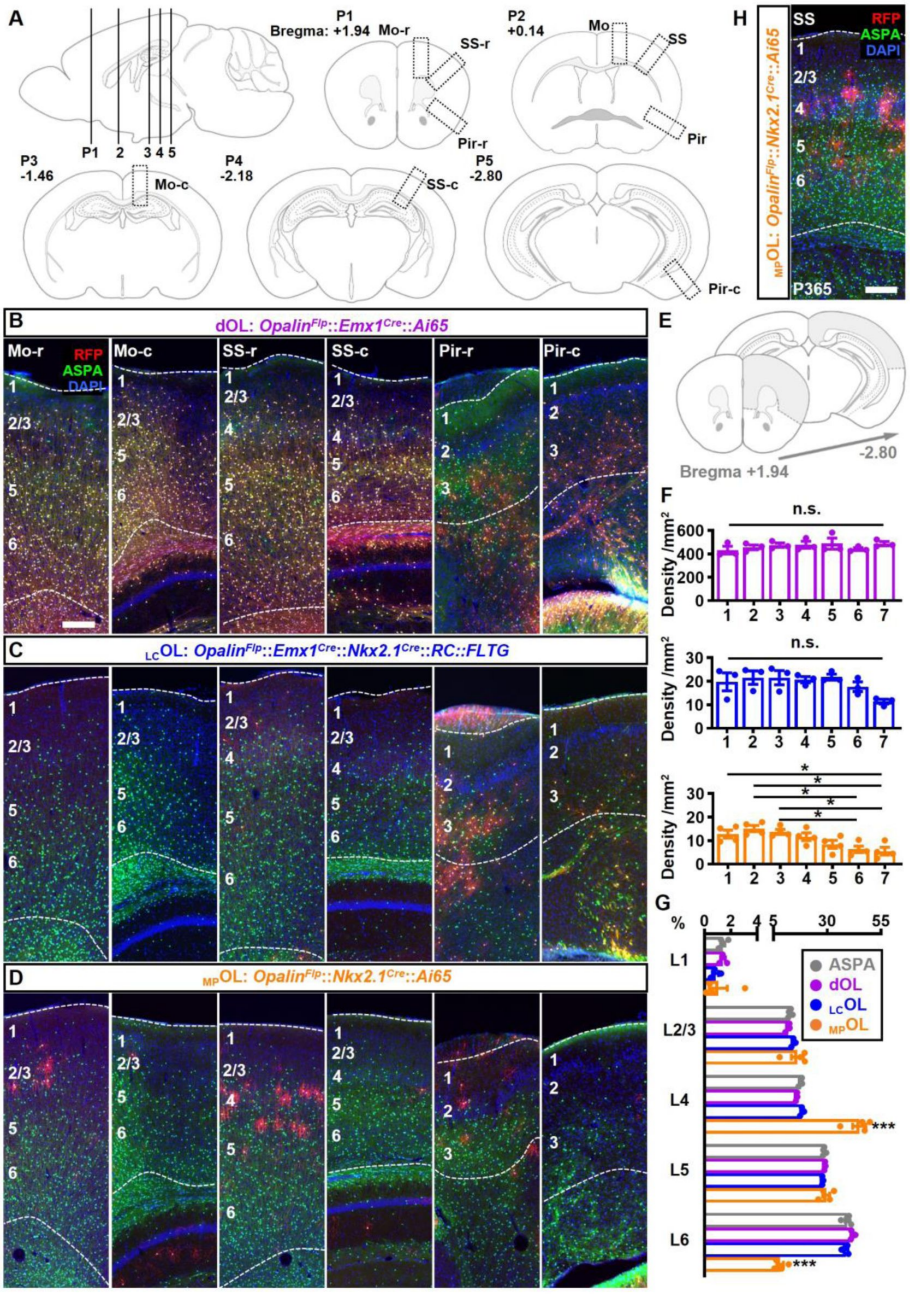

Supplementary Figure 2.

The distribution pattern of cortical dOLs, $_{MP}$OLs and $_{LC}$OLs

(**A**) Schematics of cortical regions chosen for quantifications and for showing representative images (boxed regions). Every fourth coronal section between Bregma +1.94 and –2.80 mm was analyzed. Position (P) 1 to 5 correspond to sections from which representative images were taken from. P2 corresponds to the sections shown in **Figure 2G-I**. **(B-D)** For each cortical region, two representative images at the rostral (r) and caudal(c) ends were presented for each combination. **(E-F)** Quantification of rostrocaudal distribution of neocortical (grey shaded region in E) dOLs, $_{LC}$OLs and $_{MP}$OLs. Slices were grouped into seven bins numbered rostrocaudally. Densities of dOLs and $_{LC}$OLs showed no significant change across bins, while $_{MP}$OLs exhibited lower density in more caudal regions. **(G)** Distributions of dOLs, $_{LC}$OLs and $_{MP}$OLs across 6 layers in SS. Similar to the total OL distribution quantified based on ASPA staining, more dOLs and $_{LC}$OLs reside in deeper layers. In contrast, $_{MP}$OLs are highly enriched in L4 at the cost of L6 with significant deviation from the total OLs. **(H)** Representative image of SS from 1 year old *Opalin*^{Flp}::*Nkx2.1*^{Cre}::*Ai65* mouse. Scale bar: 200 μm. n=3 for dOLs and $_{LC}$OLs; n=4 for $_{MP}$OLs and ASPA. Dots represent data from individual mice. Error bar: S.E.M. *P < 0.05, ***P < 0.001.

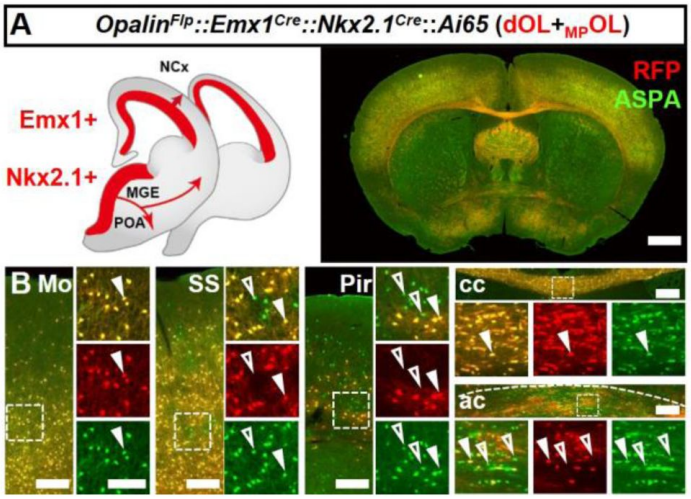

Supplementary Figure 3.

Intersectional labeling of OLs derived from both dorsal origin and MGE/POA

(**A**) Coronal sections showing both dOLs and $_{MP}$OLs labeled by RFP in *Opalin^{Flp}::Emx1^{Cre}::Nkx2.1^{Cre}::Ai65.* **(B)** Higher magnification images showing ASPA+ RFP+ dOLs/$_{MP}$OLs (closed arrow heads) and ASPA+RFP-putative $_{LC}$OLs (open arrow heads).The latter cells were difficult to find in neocortical regions such as motor cortex (Mo) and somatosensory cortex (SS), and corpus callosum (cc), but were frequently encountered in piriform cortex (Pir) and anterior commissure (ac). Scale bar: 1mm in low magnification images, 200μm in Mo, SS, cc and ac, 10 μm in high magnification images of boxed area.

References

1. Xu Q., Tam M., Anderson S.A. (2008) **Fate mapping Nkx2.1-lineage cells in the mouse telencephalon** *J Comp Neurol* **506**:16–29

2. Kessaris N., et al. (2006) **Competing waves of oligodendrocytes in the forebrain and postnatal elimination of an embryonic lineage** *Nat Neurosci* **9**:173–9

3. Gorski J.A., et al. (2002) **Cortical excitatory neurons and glia, but not GABAergic neurons, are produced in the Emx1-expressing lineage** *The Journal of neuroscience: the official journal of the Society for Neuroscience* **22**:6309–14

4. Nakahira E., et al. (2006) **Direct evidence that ventral forebrain cells migrate to the cortex and contribute to the generation of cortical myelinating oligodendrocytes** *Dev Biol* **291**:123–31

5. Tsoa R.W., et al. (2014) **Spatiotemporally different origins of NG2 progenitors produce cortical interneurons versus glia in the mammalian forebrain** *Proc Natl Acad Sci U S A* **111**:7444–9

6. Naruse M., et al. (2016) **The Dorsoventral Boundary of the Germinal Zone is a Specialized Niche for the Generation of Cortical Oligodendrocytes during a Restricted Temporal Window** *Cereb Cortex* **26**:2800–2810

7. Orduz D., et al. (2019) **Developmental cell death regulates lineage-related interneuron-oligodendroglia functional clusters and oligodendrocyte homeostasis** *Nat Commun* **10**

8. Liu R., et al. (2021) **In Vivo Clonal Analysis Reveals Development Heterogeneity of Oligodendrocyte Precursor Cells Derived from Distinct Germinal Zones** *Adv Sci (Weinh* **8**

9. Shen Z., et al. (2021) **Distinct progenitor behavior underlying neocortical gliogenesis related to tumorigenesis** *Cell Rep* **34**

10. Tripathi R.B., et al. (2011) **Dorsally and ventrally derived oligodendrocytes have similar electrical properties but myelinate preferred tracts** *J Neurosci* **31**:6809–6819

11. Winkler C.C., et al. (2018) **The Dorsal Wave of Neocortical Oligodendrogenesis Begins Embryonically and Requires Multiple Sources of Sonic Hedgehog** *J Neurosci* **38**:5237–5250

12. Zhang Y., et al. (2020) **Cortical Neural Stem Cell Lineage Progression Is Regulated by Extrinsic Signaling Molecule Sonic Hedgehog** *Cell Rep* **30**:4490–4504

13. Kippert A., et al. (2008) **Identification of Tmem10/Opalin as a novel marker for oligodendrocytes using gene expression profiling** *BMC Neurosci* **9**

14. Yoshikawa F., et al. (2008) **Opalin, a transmembrane sialylglycoprotein located in the central nervous system myelin paranodal loop membrane** *J Biol Chem* **283**:20830–40

15. Jiang W., et al. (2013) **Identification of Tmem10 as a novel late-stage oligodendrocytes marker for detecting hypomyelination** *Int J Biol Sci* **10**:33–42

16. Marques S., et al. (2016) **Oligodendrocyte heterogeneity in the mouse juvenile and adult central nervous system** *Science* **352**:1326–1329

17. Plummer N.W., et al. (2015) **Expanding the power of recombinase-based labeling to uncover cellular diversity** *Development* **142**:4385–93

18. Huang H., et al. (2023) **Immunological Markers for Central Nervous System Glia** *Neurosci Bull* **39**:379–392

19. Li J., et al. (2023) **The Lateral Ganglionic Eminence Does Not Generate Cortical Oligodendrocytes** *bioRxiv*

20. Gong L., et al. (2022) **Emerging strategies for the genetic dissection of gene functions, cell types, and neural circuits in the mammalian brain** *Mol Psychiatry* **27**:422–435

21. Madisen L., et al. (2015) **Transgenic mice for intersectional targeting of neural sensors and effectors with high specificity and performance** *Neuron* **85**:942–58

22. He M., et al. (2016) **Strategies and Tools for Combinatorial Targeting of GABAergic Neurons in Mouse Cerebral Cortex** *Neuron* **91**:1228–1243

Editors

Reviewing Editor
Samuel Pleasure
University of California, San Francisco, San Francisco, United States of America

Senior Editor
Sofia Araújo
University of Barcelona, Barcelona, Spain

Reviewer #1 (Public Review):

Summary:

In this study, the authors generated a novel transgenic mouse line OpalinP2A-Flpo-T2A-tTA2 to specifically label mature oligodendrocytes, and at the same time their embryonic origins by crossing with a progenitor cre mouse line. With this clever approach, they found that LGE/CGE-derived OLs make minimum contributions to the neocortex, whereas MGE/POA-derived OLs make a small but lasting contribution to the cortex. These findings are contradictory to the current belief that LGE/CGE-derived OPCs make a sustained contribution to cortical OLs, whereas MGE/POA-derived OPCs are completely eliminated. Thus, this study provides a revised and more comprehensive view on the embryonic origins of cortical oligodendrocytes. To specifically label mature oligodendrocytes, and at the same time their embryonic origins by crossing with a progenitor cre mouse line. With this clever approach, they found that LGE/CGE-derived OLs make minimum contributions to the neocortex, whereas MGE/POA-derived OLs make a small-but-lasting contribution to to cortex. These findings are contradictory to the current belief that LGE/CGE-derived OPCs make a sustained contribution to cortical OLs, whereas MGE/POA-derived OPCs are completely eliminated. Thus, this study has provided a revised and updated view on the embryonic origins of cortical oligodendrocytes.

Strengths:

The authors have generated a novel transgenic mouse line to specifically label mature differentiated oligodendrocytes, which is very useful for tracing the final destiny of mature myelinating oligodendrocytes. Also, the authors carefully compared the distribution of three progenitor cre mouse lines and suggested that Gsh-cre also labeled dorsal OLs, contrary to the previous suggestion that it only marks LGE-derived OPCs. In addition, the author also analyzed the relative contributions of OLs derived from three distinct progenitor domains in other forebrain regions (e.g. Pir, ac). Finally, the new transgenic mouse lines and established multiple combinatorial genetic models will facilitate future investigations of the developmental origins of distinct OL populations and their functional and molecular heterogeneity.

Comments on latest version: In this revised and improved manuscript, the authors have adequately addressed my concerns, and I have no further issues to raise.

https://doi.org/10.7554/eLife.95406.2.sa2

Reviewer #2 (Public Review):

In this manuscript, Cai et al use a combination of mouse transgenic lines to re-examine the question of the embryonic origin of telencephalic oligodendrocytes (OLs). Their tools include a novel Flp mouse for labelling mature oligodendrocytes and a number of pre-existing lines (some previously generated by the last author in Josh Huang's lab) that allowed combinatorial or subtractive labelling of oligodendrocytes with different origins. The conclusion is that cortically-derived OLs are the predominant OL population in the motor and somatosensory cortex and underlying corpus callosum, while the LGE/CGE generates OLs for the piriform cortex and anterior commissure rather than the cerebral cortex. Small numbers of MGE-derived OLs persist long-term in the motor, somatosensory and piriform cortex.

Strengths:
The strength and novelty of the manuscript lie in the elegant tools generated and used. These have enabled the resolution of the issue regarding the contribution of different telencephalic progenitor zones to the cortical oligodendrocyte population.

Comments on latest version:

The revised manuscript by Cai et al has addressed all the issues raised. I have some minor comments:

Figure 2: The y axis in figure 2L should be the same as the y axis in 2M to make the contribution to Mo and SS more clear.

Figure 3: Although this is clear in the figure, A an B should be labelled as classical model and new model to help the reader understand immediately what the two figures show.

Suppl Fig 2: It is not clear what 1-7 represent. It should be made clear in the legend which areas have been pooled into the different bins. The X axis should be labelled.

https://doi.org/10.7554/eLife.95406.2.sa1

Reviewer #3 (Public Review):

In the manuscript entitled "Embryonic Origins of Forebrain Oligodendrocytes Revisited by Combinatorial Genetic Fate Mapping," Cai et al. used an intersectional/subtractional strategy to genetically fate-map the oligodendrocyte populations (OLs) generated from medial

ganglionic eminence (NKX2.1+), lateral ganglionic eminences, and dorsal progenitor cells (EMX1+). Specifically, they generated an OL-expressing reporter mouse line OpalinP2A-Flpo-T2A-tTA2 and bred with region-specific neural progenitor-expressing Cre lines EMX1-Cre for dOL and NKX2.1-Cre for MPOL. They used a subtractional strategy in the OpalinFlp::Emx1Cre::Nkx2.1Cre::RC::FLTG mouse line to predict the origins of OLs from lateral/caudal ganglionic eminences (LC). With their genetic tools, the authors concluded that neocortical OLs primarily consist of dOLs. Although the populations of OLs (dOLs or MP-OLs) from Emx1+ or Nkx2.1+ progenitors are largely consistent with previous findings, they observed that MP-OLs contribute minimally but persist into adulthood without elimination as in the previous report (PMID: 16388308).

Intriguingly, by using an indirect subtraction approach, they hypothesize that both Emx1-negative and Nkx2.1-negative cells represent the progenitors from lateral/caudal ganglionic eminences (LC), and conclude that neocortical OLs are not derived from the LC region. This is in contrast to the previous observation for the contribution of LC-expressing progenitors (marked by Gsx2-Cre) to neocortical OLs (PMID: 16388308). The authors claim that Gsh2 is not exclusive to progenitor cells in the LC region (PMID: 32234482). However, Gsh2 exhibits high enrichment in the LC during early embryonic development. The presence of a small population of Gsh2-positive cells in the late embryonic cortex could originate/migrate from Gsh2-positive cells in the LC at earlier stages (PMID: 32234482). Consequently, the possibility that cortical OLs derived from Gsh2+ progenitors in LC could not be conclusively ruled out. Notably, a population of OLs migrating from the ventral to the dorsal cortical region was detected after eliminating dorsal progenitor-derived OLs (PMID: 16436615).

The indirect subtraction data for LC progenitors drawn from the OpalinFlp-tdTOM reporter in Emx1-negative and Nkx2.1-negative cells in the OpalinFlp::Emx1Cre::Nkx2.1Cre::RC::FLTG mouse line present some caveats that could influence their conclusion. The extent of activity from the two Cre lines in the OpalinFlp::Emx1Cre::Nkx2.1Cre::RC::FLTG mice remains uncertain. The OpalinFlp-tdTOM expression could occur in the presence of either Emx1Cre or Nkx2.1Cre, raising questions about the contribution of the individual Cre lines. To clarify, the authors should compare the tdTOM expression from each individual Cre line, OpalinFlp::Emx1Cre::RC::FLTG or OpalinFlp::Nkx2.1Cre::RC::FLTG, with the combined OpalinFlp::Emx1Cre::Nkx2.1Cre::RC::FLTG mouse line. This comparison is crucial as the results from the combined Cre lines could appear similar to only one Cre line active.

Overall, the authors provided intriguing findings regarding the origin and fate of oligodendrocytes from different progenitor cells in embryonic brain regions. However, further analysis is necessary to substantiate their conclusion about the fate of LC-derived OLs convincingly.

Comments on latest version: The overall responses by the authors are satisfactory.

https://doi.org/10.7554/eLife.95406.2.sa0

Author response:

The following is the authors' response to the original reviews.

> ***Reviewer #1 (Public Review):***
>
> *Summary:*
>
> *In this study, the authors generated a novel transgenic mouse line OpalinP2A-Flpo-T2A-tTA2 to specifically label mature oligodendrocytes, and at the same time their embryonic origins by crossing with a progenitor cre mouse line. With this clever approach, they*

> *found that LGE/CGE-derived OLs make minimum contributions to the neocortex, whereas MGE/POA-derived OLs make a small but lasting contribution to the cortex. These findings are contradictory to the current belief that LGE/CGE-derived OPCs make a sustained contribution to cortical OLs, whereas MGE/POA-derived OPCs are completely eliminated. Thus, this study provides a revised and more comprehensive view on the embryonic origins of cortical oligodendrocytes. To specifically label mature oligodendrocytes, and at the same time their embryonic origins by crossing with a progenitor cre mouse line. With this clever approach, they found that LGE/CGE-derived OLs make minimum contributions to the neocortex, whereas MGE/POA-derived OLs make a small-but-lasting contribution to to cortex. These findings are contradictory to the current belief that LGE/CGE-derived OPCs make a sustained contribution to cortical OLs, whereas MGE/POA-derived OPCs are completely eliminated. Thus, this study has provided a revised and updated view on the embryonic origins of cortical oligodendrocytes.*
>
> *Strengths:*
>
> *The authors have generated a novel transgenic mouse line to specifically label mature differentiated oligodendrocytes, which is very useful for tracing the final destiny of mature myelinating oligodendrocytes. Also, the authors carefully compared the distribution of three progenitor cre mouse lines and suggested that Gsh-cre also labeled dorsal OLs, contrary to the previous suggestion that it only marks LGE-derived OPCs. In addition, the author also analyzed the relative contributions of OLs derived from three distinct progenitor domains in other forebrain regions (e.g. Pir, ac). Finally, the new transgenic mouse lines and established multiple combinatorial genetic models will facilitate future investigations of the developmental origins of distinct OL populations and their functional and molecular heterogeneity.*
>
> *Weaknesses:*
>
> *Since OpalinP2A-Flpo-T2A-tTA2 only labels mature oligodendrocytes but not OPCs, the authors can not suggest that the lack of LGE/CGE-derived-OLs in the neocortex is less likely caused by competitive postnatal elimination, but more likely due to limited production and/or allocation (line 118-9). It remains possible that LGE/CGE-derived OPCs migrate into the cortex but are later eliminated.*

We are glad that the reviewer appreciates our work and are grateful for the positive comments and the constructive suggestion. We agree with the reviewer that our methodology by itself cannot suggest whether the lack of LGE/CGE-derived-OLs in the neocortex is caused by competitive postnatal elimination or not. That is why we cited a parallel work by Li et al. (ref [17] in the original manuscript; ref [19] in the revised manuscript), in which in utero electroporation (IUE) failed to label LGE-derived OL lineage cells in both embryonic and early postnatal brains. Although they did not directly explore CGE using IUE, their fate mapping results using Emx1-Cre; Nkx2.1-Cre; H2B-GFP at P0 and P10 revealed very low percentage of LGE/CGE-derived OL lineage cells. The lack of adult labeling in our study together with the lack of developmental labeling in the other study prompted us to hypothesize that the lack of LGE/CGE-derived-OLs in the neocortex is less likely caused by competitive postnatal elimination, but more likely due to limited production and/or allocation. In the revised manuscript, we have expanded the discussion to explain this point more clearly.

> ***Reviewer #2 (Public Review):***
>
> *Summary:*
>
> *In this manuscript, Cai et al use a combination of mouse transgenic lines to re-examine the question of the embryonic origin of telencephalic oligodendrocytes (OLs). Their tools include a novel Flp mouse for labelling mature oligodendrocytes and a number of pre-*

> *existing lines (some previously generated by the last author in Josh Huang's lab) that allowed combinatorial or subtractive labelling of oligodendrocytes with different origins. The conclusion is that cortically-derived OLs are the predominant OL population in the motor and somatosensory cortex and underlying corpus callosum, while the LGE/CGE generates OLs for the piriform cortex and anterior commissure rather than the cerebral cortex. Small numbers of MGE-derived OLs persist long-term in the motor, somatosensory and piriform cortex.*
>
> *Strengths:*
>
> *The strength and novelty of the manuscript lies in the elegant tools generated and used and which have the potential to elegantly and accurately resolve the issue of the contribution of different progenitor zones to telencephalic regions.*

We are glad that the reviewer appreciates our work and are grateful for the overall positive comments.

> *Weaknesses:*
>
> *(1) Throughout the manuscript (with one exception, lines 76-78), the authors quantified OL densities instead of contributions to the total OL population (as a % of ASPA for example). This means that the reader is left with only a rough estimation of the different contributions.*

We thank the reviewer for this constructive suggestion. We have replaced the density quantification (Figure 2F and 3D in the original manuscript) with contributions to the total OL population (% of ASPA) (Figure 2J and 2N in the revised manuscript).

> *(2) All images and quantifications have been confined to one level of the cortex and the potential of the MGE and the LGE/CGE to produce oligodendrocytes for more anterior and more posterior cortical regions remains unexplored.*

The quantifications were not confined to one level of the cortex but were performed in brain sections ranging from Bregma +1.94 to -2.80 mm, as shown in Supplementary Figure 2A-B in the original manuscript. We apologize for not having stated and presented this information clearly enough, and for the confusions it may have caused. In the revised manuscript, we have added relevant descriptions in the “Material and Methods” section (line 199-200*) and schematics along with representative images of more anterior and more posterior cortical regions (Supplementary Figure 2A-D).

> *(3) Hence, the statement that "In summary, our findings significantly revised the canonical model of forebrain OL origins (Figure 4A) and provided a new and more comprehensive view (Figure 4B)." (lines 111, 112) is not really accurate as the findings are neither new nor comprehensive. Published manuscripts have already shown that (a) cortical OLs are mostly generated from the cortex [Tripathi et al 2011 (https://doi.org/10.1523/JNEUROSCI.6474-10.2011), Winker et al 2018 (https://doi.org/10.1523/JNEUROSCI.3392-17.2018) and Li et al (https://doi.org/10.1101/2023.12.01.569674)] and (b) MGE-derived OLs persist in the cortex [Orduz et al 2019 (https://doi.org/10.1038/s41467-019-11904-4) and Li et al 2024 (https://doi.org/10.1101/2023.12.01.569674)]. Extending the current study to different rostro-caudal regions of the cortex would greatly improve the manuscript.*

As explained in the response to comment (2), our original quantifications included different rostro-caudal regions of the cortex. In the revised manuscript, we have added more

schematics and representative images in the Supplementary Figure 2 for better illustration to resolve the concern of comprehensiveness.

We thank the reviewer for listing and summarizing highly relevant published researches along with the parallel study by Li et al. submitted to eLife. We apologize for the omission of the first two references in our original manuscripts and have cited them in appropriate places (ref [10] and ref [11] in the revised manuscript). However, we believe these works do not compromise the novelty and significance of our work for the following reasons:

(1) Tripathi et al. 2011 (ref [10] in the revised manuscript) analyzed OL lineage cells in the corpus callosum and the spinal cord, but not in the cortex and anterior commissure. Their analysis was performed in juvenile mice (P12/13), not in adulthood. Most importantly, their analysis of ventrally derived OL lineage cells relied on lineage tracing using Gsh2Cre, which in fact also label OLs derived from Gsh2+ dorsal progenitors. In contrast, we analyzed mature OLs in the cortex, corpus callosum and anterior commissure in 2-month-old adult mice. We used intersectional and subtractive strategy to label OLs derived from dorsal, LGE/CGE and MGE/POA origins. Our strategy differentiated the two different ventral lineages (LGE/CGE vs. MGE/POA) and avoided mixed labeling of OLs from ventral and dorsal Gsh2+ progenitors.

(2) Winkler et al. 2018 (ref [11] in the revised manuscript) analyzed OLs derived from dorsal progenitors but only quantified those in the gray matter and the white matter of somatosensory cortex. Their quantification relied on co-staining with Olig2/Sox10, and thereby included both oligodendrocyte precursors (OPCs) and OLs. In contrast, we analyzed mature OLs from three origins and quantified not only neocortical regions (Mo and SS) but also an archicortical region (Pir). Our analysis revealed that although dorsally derived OLs dominate neocortex, ventrally derived OLs, especially the LGE/CGE-derived ones, dominate piriform cortex.

(3) Orduz et al. 2019 (ref [7] in the original manuscript and the revised manuscript) mainly focused on POA-derived OLs in the somatosensory cortex. Although they performed limited analysis on MGE/POA-derived OPCs at postnatal day 10 and 19, no quantification of MGE/POA-derived OLs was performed in terms of their density, contribution to the total OL population and spatial distribution in the cortex. In contrast, we performed systematic quantification on these aspects to demonstrate that MGE/POA-derived OLs make small but sustained contribution to cortex with a distribution pattern distinctive from those derived from the dorsal origin.

(4) Li et al. 2024 (ref [17] in the original manuscript and [19] in the revised manuscript) is a parallel study submitted to eLife. Their and our independent discoveries nicely complemented each other. Using different sets of techniques and experiments but some shared genetic mouse models, we both found that LGE/CGE made minimum contribution to neocortical OLs. Their analysis in the prenatal and early postnatal stages together with our analysis in the adult brain painted a more comprehensive picture of cortical oligodendrogenesis. The uniqueness of our work is that we performed systematic quantification of all three origins and uncovered the differential contributions to neocortex, piriform cortex, corpus callosum and anterior commissure.

In summary, our work developed novel strategies to faithfully trace OLs from the three different origins and performed systematic analysis in the adult brain. Our data uncovered their differential contributions to neocortex, piriform cortex and the two commissural white matter tracts, which significantly differ not only from the canonical view but also from other previous studies in aspects discussed above. We believe our discoveries did significantly revise the canonical model of forebrain OL origins and provided a new and more comprehensive view.

Reviewer #3 (Public Review):

In the manuscript entitled "Embryonic Origins of Forebrain Oligodendrocytes Revisited by Combinatorial Genetic Fate Mapping," Cai et al. used an intersectional/subtractional strategy to genetically fate-map the oligodendrocyte populations (OLs) generated from medial ganglionic eminence (NKX2.1+), lateral ganglionic eminences, and dorsal progenitor cells (EMX1+). Specifically, they generated an OL-expressing reporter mouse line OpalinP2A-Flpo-T2A-tTA2 and bred with region-specific neural progenitor-expressing Cre lines EMX1-Cre for dOL and NKX2.1-Cre for MPOL. They used a subtractional strategy in the OpalinFlp::Emx1Cre::Nkx2.1Cre::RC::FLTG mouse line to predict the origins of OLs from lateral/caudal ganglionic eminences (LC). With their genetic tools, the authors concluded that neocortical OLs primarily consist of dOLs. Although the populations of OLs (dOLs or MP-OLs) from Emx1+ or Nkx2.1+ progenitors are largely consistent with previous findings, they observed that MP-OLs contribute minimally but persist into adulthood without elimination as in the previous report (PMID: 16388308).

Intriguingly, by using an indirect subtraction approach, they hypothesize that both Emx1-negative and Nkx2.1-negative cells represent the progenitors from lateral/caudal ganglionic eminences (LC), and conclude that neocortical OLs are not derived from the LC region.The authors claim that Gsh2 is not exclusive to progenitor cells in the LC region (PMID: 32234482). However, Gsh2 exhibits high enrichment in the LC during early embryonic development. The presence of a small population of Gsh2-positive cells in the late embryonic cortex could originate/migrate from Gsh2-positive cells in the LC at earlier stages (PMID: 32234482). Consequently, the possibility that cortical OLs derived from Gsh2+ progenitors in LC could not be conclusively ruled out. Notably, a population of OLs migrating from the ventral to the dorsal cortical region was detected after eliminating dorsal progenitor-derived OLs (PMID: 16436615).

The indirect subtraction data for LC progenitors drawn from the OpalinFlp-tdTOM reporter in Emx1-negative and Nkx2.1-negative cells in the OpalinFlp::Emx1Cre::Nkx2.1Cre::RC::FLTG mouse line present some caveats that could influence their conclusion. The extent of activity from the two Cre lines in the OpalinFlp::Emx1Cre::Nkx2.1Cre::RC::FLTG mice remains uncertain. The OpalinFlp-tdTOM expression could occur in the presence of either Emx1Cre or Nkx2.1Cre, raising questions about the contribution of the individual Cre lines. To clarify, the authors should compare the tdTOM expression from each individual Cre line, OpalinFlp::Emx1Cre::RC::FLTG or OpalinFlp::Nkx2.1Cre::RC::FLTG, with the combined OpalinFlp::Emx1Cre::Nkx2.1Cre::RC::FLTG mouse line. This comparison is crucial as the results from the combined Cre lines could appear similar to only one Cre line active.

Overall, the authors provided intriguing findings regarding the origin and fate of oligodendrocytes from different progenitor cells in embryonic brain regions. However, further analysis is necessary to substantiate their conclusion about the fate of LC-derived OLs convincingly.

We thank the reviewer for these thoughtful comments. We agree with the reviewer that the presence of Gsh2-positive cells in the late embryonic cortex by itself could not rule out the possibility that they originate/migrate from Gsh2-positive cells in the LC at earlier stages. Staining dorsal-lineage intermediate progenitors with Gsh2, or performing intersectional lineage tracing using Gsh2Cre along with a dorsal-specific Flp driver, would provide more direct evidence on this issue. Nonetheless, as our lineage tracing of LGE/CGE-derive OLs did not employ Gsh2Cre, the doubt on the identity of Gsh2+ cortical progenitors should not affect the interpretation of our data.

Regarding the subtractional LCOL labeling strategy used in our study, we wonder if there was any misunderstanding by the reviewer. As stated in our manuscript (line 59-61) and reiterated by the reviewer, OpalinFlp::Emx1Cre::Nkx2.1Cre::RC::FLTG labels OLs derived from progenitors that express neither Emx1Cre nor Nkx2.1Cre. As these two progenitor pools do not overlap with each other, there is a purely additive effect of their actions. If there is any concern about efficiency and specificity, it would be non-adequate Cre-mediated recombinations that lead to mislabeling of dOLs or MPOLs as LCOLs (i.e., OLs derived from Emx1 or Nkx2.1-expressing progenitors were not successfully "subtracted" and thereby "wrongly" retained RFP expression). Therefore, the bona-fide LGE/CGE-derive OLs would only be fewer but not more than RFP+ LCOLs labeled by our subtractional strategy, even if any of the Cre lines did not work efficiently enough. In any case, this would not affect our conclusion that LGE/CGE-derive OLs make a minimal contribution to neocortex, as the "ground truth" contribution by LGE/CGE could only be less but not more than what we have observed using the current strategy.

In support of our conclusion, a parallel study by Li et al. 2024 (ref [17] in the original manuscript; ref [19] in the revised manuscript) also provided independent experimental evidence that "any contribution of oligodendrocyte precursors to the developing cortex from the lateral ganglionic eminence is minimal in scope (quoted from its eLife assessment)." In addition, in their revision, they performed Gsh2 immunostaining in P0 Emx1Cre::HG-loxP mouse and found nearly all Gsh2+ cells in the cortical SVZ were derived from the Emx1+ lineage. We are glad that this additional piece of evidence further clarified the case, but still want to emphasize that the subtractional strategy we took was designed purposefully to avoid the potential uncertainty of Gsh2Cre and to more faithfully label LGE/CGE-derived OLs. Therefore, the validity of our conclusion about the fate of LC-derived OLs should be independent from the question on the identity of Gsh2+ cortical progenitors and stands well by itself.

We hope that these explanations have adequately addressed the reviewer's concerns.

> ***Recommendations for the authors:***
>
> ***Reviewer #2 (Recommendations For The Authors):***
>
> *In Figures 2C, 2D, 2E and 3D, the authors should provide counts of labelled cells as a % of ASPA+ cells. This will give an accurate picture of the contribution of the different progenitor regions to OLs.*
>
> *The graphs in Figure 2F are unnecessary since they are simply repeats of C-E but re-arranged.*

We thank the reviewer for the valuable suggestions. These two recommendations are sort of related, and thereby we made the following changes. We replaced the density quantification in Figure 2F and 3D with % of ASPA (Figure 2J and 2N in the revised manuscript) to give an accurate picture of the contribution of the different progenitor regions to OLs, as suggested by the reviewer. We still retained the density counts in Figure 2C-E (Figure 2G-I in the revised manuscript). Together with quantifications of rotral-caudal and larminar distributions presented in Supplementary Figure 2, these data demonstrated that OLs from differential origins display distinct spatial distribution patterns.

> *At what ages were the quantifications performed in all the figures?*

We apologize for the omission of this information in the original manuscript. All quantifications were performed in 2-month-old adult mice. We have added this information in the "Material and Methods" section of the revised manuscript.

> *In 2D, and 3B the GFP should have been activated but the authors do not show it or quantify it presumably because GFP would flood the sections in the presence of Emx1Cre. Nevertheless, since eGFP is shown in the diagram in 2B, the authors should mention why they chose not to show it.*

We thank the reviewer for the helpful comment and the suggestion. We have modified the schematic in Figure 2B and added explanation in the figure legend (line 308-313). We also added a schematic in Supplementary Figure 1A along with images of GFP channel in Supplementary Figure 1D (line 338-350).

> *All the main figures and supplementary figures are too small to see properly.*

We are sorry that there was severe compression of images in the combined manuscript file at the conversion step during the initial submission. We apologize for the compromised image quality and have re-uploaded full-size figures as individual files on BioRxiv soon after receiving the reviews. For the revised manuscript, we also take care to upload full-size figures at high resolution as individual files to ensure their quality of presentation.

> *Supplementary Figure 2E is unnecessary and perhaps misleading the reader that cortical-derived OLs have a preference for the lower layers whereas the distribution may simply reflect the distribution of OLs in the cortex.*

We thank the reviewer for the helpful comment and the suggestion. We have removed this panel and replaced it with quantifications of relative laminar distributions of the total (ASPA+) OLs along with those from the three different origins (Supplementary Figure 2G in the revised manuscript). Indeed, the preference for the lower layers of dorsally-derived OLs mirrored the distribution of total OLs in the cortex, while the MGE/POA-derived OLs deviate significantly from others and exhibit higher preference towards layer 4.

> *Quantification of labelled cells as a % of ASPA should also be performed in Supplementary Figure 3.*

We thank the reviewer for this suggestion. In the revised manuscript, we have included quantifications of labelled cells as % of ASPA for both OpalinFlp::Emx1Cre::Ai65 and OpalinFlp::Nkx2.1Cre::Ai65 (Figure 2J and N). The sum of the these two data sets will be equivalent to those of OpalinFlp::Emx1Cre::Nkx2.1Cre::Ai65 shown in Supplementary Figure 3, and thereby we did not perform additional quantifications to avoid redundant efforts.

> *Imaging and quantification should be extended to more posterior regions of the cortex to find out whether the contribution is different from the areas already examined.*

We thank the reviewer for the suggestion on imaging and apologize for the confusion about the range of quantification. As explained in the response to comment (2) of weakness, the quantifications were not confined to one level of the cortex but were performed in brain sections ranging from Bregma +1.94 to -2.80 mm, as shown in Supplementary Figure 2A-B in the original manuscript. In the revised manuscript, we have added relevant descriptions in the “Material and Methods” section (line 199-200) and schematics along with representative images of more anterior and more posterior cortical regions (Supplementary Figure 2A-D).

> ***Reviewer #3 (Recommendations For The Authors):***
>
> *(1) The authors should provide Opalin reporter expression data across various brain regions at different developmental stages to clarify the expression pattern of the*

> *reporter.*

We appreciate the reviewer's comment. We chose to performed all quantifications in adult mice as Opalin is a well-established marker for differentiated OLs and the recombinase-dependent reporter expression is accumulative and irreversible. If there is any non-specific labeling in any earlier developmental stage, it would be retained and manifested at the timepoint we examined as well. In another word, the fact that we did not detect any non-specific labeling in the current dataset but only confined labeling in mature OLs ensured that no non-OL labeling was present in earlier timepoint. As shown in Figure 1D-F, reporter expression activated by the Opalin driver is presented at high OL specificity in all analyzed brain regions. This is further corroborated by results from combinatorically labeled samples (Figure 2 and Supplementary Figure 2), in which only OLs but not any other cell types were labeled in all analyzed brain regions too. Following the reviewers' suggestions, we have added representative images of more rostral and more caudal cortical regions (Supplementary Figure 2B-D), which also showed highly specific OL labeling.

> *(2) In Figure 1D, please specify the developmental stage of the mice used for staining.*

We apologize for the omission of this information in the original manuscript. All quantifications were performed in 2-month-old adult mice. We have added this information in the "Material and Methods" section (line 199-200) of the revised manuscript.

> *(3) The authors should clarify if the Opalin reporter expressed in OPCs and astrocytes at developmental stages of mice, such as P0, P7, and P30.*

We appreciate the reviewer's comment, but as explained in response to comment (1), Opalin is a well-established marker for differentiated OLs which is not expressed in OPCs or astrocytes. As shown in Figure 1D-E, reporter expression is confined to CC1+ differentiated OLs with no colocalization with Sox9 (astrocyte marker). In support with this observation, only ASPA+ differentiated OLs but no OPC or astrocyte were labeled in any of the combinatorial lineage tracing samples generated using this line combined with progenitor-Cre lines. In addition to marker staining, we also did not observe any RFP+ cells with OPC or astrocyte morphology. As the recombinase-dependent reporter expression is accumulative and irreversible, the fact no non-specific labeling was observed in adult brain retrospectively proved the specificity of Oplain-Flp in earlier developmental stages.

> *(4) In Figure 1E, authors should address why the efficiency of the tdTomato line is notably lower compared to that of H2B-GFP and whether the stability of reporters could impact the conclusions drawn.*

The difference in reporting efficiency is mainly caused by differences inherent to the two reporting systems. The TRE-RFP reporter is derived from Ai62, composed of a Tet response element and tdTomato inserted into the T1 TIGRE locus. The tdTomato expression is driven by tTA-TRE transcriptional activation. The HG-loxP reporter is derived from HG-Dual, composed of a CAG promoter, a frt-flanked STOP cassette, and H2B-GFP inserted into the Rosa26 locus. The H2B-GFP expression is driven by CAG promoter after Flp-mediated removal of the STOP cassette. A Flp-dependent tdTomato reporter designed in the same way as the HG-FRT reporter would have similar efficiency. In fact, the RC::FLTG reporter can be viewed as such a reporter in the absence of Cre, which did show similarly high efficiency as HG-FRT and supported efficient subtractive labeling of LGE/CGE-derived OLs. We apologize for a typo in the title of the Y-axis of the right panel in the original Figure 1F which may have caused potential misunderstanding. The "RFP+CC1+/CC1" should be "XFP+CC1/CC1". We have corrected this mistake and revised the figure legend for clearer description of the data (Line 293-302 in the revised manuscript).

> *(5) In Figure 2, please clarify the developmental stage of the mice used for staining. Authors should present the eGFP image in addition to tdTOM.*

We apologize for the omission of the age information in the original manuscript. All quantifications were performed in 2-month-old adult mice. We have added this information in the "Material and Methods" section (line 199-200) of the revised manuscript. We thank the reviewer for the suggestion on eGFP image and have presented it in supplementary Figure 1 in the revised manuscript.

(6) in Figure 2D, authors should display the eGFP image alongside the tdTomato image. It is difficult to assess the efficiency of Emx-Cre and Nkx2.1-Cre.

We thank the reviewer for the suggestion on eGFP image and have presented eGFP image in Supplementary Figure 1D in the revised manuscript. There are two reasons why we chose to present it in the supplementary figure instead of main figure. First, we added ASPA staining in the green channel along with quantifications of RFP cells as % of ASPA in Figure 2 in the revised manuscript, following reviewer #2's suggestion. Second, as pointed out by reviewer #2, GFP would flood the sections in the presence of Emx1Cre and could be quite distractive if it was shown together with RFP.

We were not entirely sure what exactly the reviewer means by "assess the efficiency of Emx-Cre and Nkx2.1-Cre", but we believe that the quantifications of RFP cells as % of ASPA clarified the contribution of each origin to the total OLs (Figure 2J and 2N in the revised manuscript).

> *(7) Figure 3 depicts the entire brain, replicating the image presented in Figure 2. It would be beneficial to consolidate Figures 2 and 3, as they showcase identical brain scans of different regions.*

We thank the reviewer for the constructive suggestion and have consolidated Figures 2 and 3 in the original manuscript into Figure 2 in the revised manuscript.

https://doi.org/10.7554/eLife.95406.2.sa4